

**Calculations guide a practical way to synthesize N8
polymeric nitrogen from N3- precursor**

Journal:	<i>Physical Chemistry Chemical Physics</i>
Manuscript ID	CP-ART-11-2020-006053
Article Type:	Paper
Date Submitted by the Author:	22-Nov-2020
Complete List of Authors:	Alzaim, Safa; New Jersey Institute of Technology, Department of chemical and materials engineering Wu, Zhiyi; New Jersey Institute of Technology, Department of chemical and materials engineering Benchafia, El mostafa; New Jersey Institute of Technology, Department of Physics Young, Joshua; New Jersey Institute of Technology, Department of chemical and materials engineering wang, xianqin; New Jersey Institute of Technology, Department of chemical and materials engineering

SCHOLARONE™
Manuscripts



Thank you very much for your agreeing to review this manuscript for [Physical Chemistry Chemical Physics \(PCCP\)](#).

PCCP is an international journal for the publication of cutting-edge original work in physical chemistry, chemical physics and biophysical chemistry. To be suitable for publication in PCCP, articles must include significant innovation and/or insight into physical chemistry; this is the most important criterion that reviewers and the Editors will judge against when evaluating submissions. Further information on our scope can be found at rsc.li/pccp.

PCCP's Impact Factor is **3.430** (2019 Journal Citation Reports®)

The following manuscript has been submitted for consideration as a
PAPER

Full papers should contain original scientific work that has not been published previously. Full papers based on Communications are encouraged provided that they represent a substantial extension of the original material. There are no restrictions on the length of a paper. Authors should include a brief discussion in the Introduction that sets the context for the new work and gives their motivation for carrying out the study.

When preparing your report, please:

- Focus on the originality, importance, impact and reliability of the science. English language and grammatical errors do not need to be discussed in detail, except where it impedes scientific understanding.
- Use the [journal scope and expectations](#) to assess the manuscript's suitability for publication in PCCP.
- State clearly whether you think the article should be accepted or rejected and include details of how the science presented in the article corresponds to publication criteria.
- Inform the Editor if there is a conflict of interest, a significant part of the work you cannot review with confidence or if parts of the work have previously been published.

Best regards,

Professor David Rueda

Editorial Board Chair

Imperial College London, UK

Dr Anna Simpson

Executive Editor

Royal Society of Chemistry

[Contact us](#)

Please visit our [reviewer hub](#) for further details of our processes, policies and reviewer responsibilities as well as guidance on how to review, or click the links below.



What to do
when you
review



Reviewer
responsibilities



Process &
policies

Calculations guide a practical way to synthesize N₈ polymeric nitrogen from N₃⁻ precursor

Safa Alzaim, Zhiyi Wu, Mostafa Benchaia, Joshua Young,* Xianqin Wang*

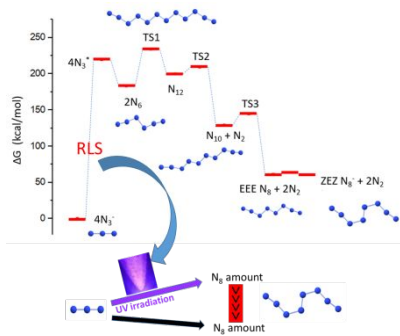
Dept. of Chemical and Materials Engineering, New Jersey Institute of Technology, Newark, NJ, 07102, USA

Corresponding author: jyoung@njit.edu; xianqin.wang@njit.edu

ABSTRACT

Polymeric nitrogen (PN) is a general family of materials containing all-nitrogen molecules or clusters. Although it is rare and challenging to synthesize PN materials, they are attracting increasing scientific attention due to their high energy storage capacity and potential use as a green catalyst. A few theoretical calculations predicted the possible PN phases from N₂ gas, but they all require extremely high pressure and temperature to synthesize. In this work, a practical way to synthesize N₈ from N₃⁻ precursor is elucidated using density functional theory calculations. The detailed synthesis mechanism, 4N₃⁻ → 4N₃^{*} → 2N₆ → N₁₂ → N₁₀ + N₂ → N₈ (ZEZ) + 2N₂, is determined. The calculated energy barriers indicate the first step (4N₃⁻ → 4N₃^{*}) is the rate-limiting step. The result guides us to rationally synthesize N₈ under UV (254nm) irradiation. As expected, UV enhances N₈ yield by nearly four times. This provides an interesting route to scalable synthesis of high energy density N₈ compounds.

TOC Graphics



KEYWORDS N₈ synthesis mechanism, Density functional theory, UV irradiation, Rate limiting step, Rational design

1. Introduction

Atmospheric nitrogen (N_2) is a diatomic molecule consisting of an extremely strong N-N triple bond. With a bond energy of 954 kJ/mol, it is one of the strongest bonds in nature^{1, 2}. Moreover, there is a very large difference in energy between this bond and the nitrogen single bond (160 kJ/mol) and double bond (418 kJ/mol).² The five outermost valence electrons of nitrogen enables network, layer and chain structures; the chains of polymeric nitrogen (PN) are of particular interest for their energy storage capacity.² The high stability of N_2 in comparison to PN accounts for the high energy release upon the conversion of PN to N_2 , and the high energy storage within a polymer chain of single bonds. These properties make these PN compounds high energy-density materials, with an energy density about three times that of TNT.² Further, decomposition to nitrogen gas does not harm the environment.¹ The high energy-density is advantageous in propellants or explosives,³ but all of these characteristics, from the ability to form many different configurations to catalytic properties, make PN appealing in applications from energy storage to catalysis⁴.

Unfortunately, transforming N_2 to stable PN compounds requires enormous temperature and pressure, and the compounds are then only stable in extreme conditions. Many experiments have produced various phases of PN, at high temperature and pressure conditions^{5,6,7}. However, these temperatures and pressures are not practical for scalability.

In recent years *ab initio* techniques have been utilized to find more efficient, effective and practical ways of synthesizing PN chains. In particular, the aforementioned problems with extreme conditions are one reason that computational methods are gaining increasing attention. In 2008, H Abou-Rachid *et al.* used *ab initio* methods to predict that armchair EZE N_8 within carbon nanotubes (CNT) would be stable in ambient conditions.⁸ In 2009, Ji *et al.* found the formation energy and transition state from N_2 for this N_8 in CNT.⁹ Also in 2009, Timoshevskii *et al.* found through *ab initio* methods that armchair N_8 on a graphene substrate would be stable in ambient conditions.¹⁰ In 2018, S Niu *et al.* computed the ambient stability of a 3D graphene/PN/graphene crystal system.² These studies demonstrated the contribution of the substrate to PN stability at ambient conditions.

In 2014, B Hirshberg *et al.* predicted through computational methods that coupled zigzag EEE and EZE N_8 would be stable at ambient conditions.¹¹ In 2018, Battaglia *et al.*¹² calculated the dissociation energies for both N_8 EEE and EZE isomers (as defined in Reference¹³) to $N_6 +$

N_2 and $2\text{N}_3 + \text{N}_2$. They noted that the EEE isomer had a lower interaction energy and was geometrically more linear. This geometry would make the N_8 more capable of confinement in a CNT without distortion, and so steric effects might dictate mechanism pathways.

Another route to produce PN is through photolysis of azide to produce radical N_3^* . This approach was studied by Barat *et al.*¹⁴ and Treinin *et al.*¹⁵ in 1969 as well as Hayon *et al.*¹⁶ in 1970. They identified the absorption spectra associated with the N_3^* formation from N_3 . In 2016, Peiris *et al.*¹⁷ explored the photolysis of polynitride materials at 4.8 to 8.1 GPa of pressure. On the other hand, an experiment by Holtgrewe *et al.*¹⁸ used photochemistry to synthesize PN at high pressure; however, their products were not clearly identified. This potential route to PN compounds still remains relatively unexplored.

However, in 2014, Wu *et al.*¹⁹ successfully synthesized N_8^- under ambient conditions and found it to be a highly active oxygen reduction reaction (ORR) catalyst.¹⁹ Unlike conventional PN fabrications, which used N_2 precursors in diamond-anvil cell systems, the group used an azide precursor. The azide precursor meant obviating the high temperature and pressure required to change the bonding in N_2 . The azide was subjected to cyclic voltammetry (CV), in which a potential was swept and the resulting current measured. The process was performed in ambient conditions and produced stable N_8 PN chains. However, the synthesis mechanism of $\text{N}_3^- \rightarrow \text{N}_8$ remains unclear. In this work, density functional theory (DFT) calculations are used to determine the probable pathway for the production of EZE N_8 from azide in ambient conditions.

2. Methods

All calculations were performed using ORCA²⁰ quantum chemistry software. All geometries were optimized with DFT, utilizing the B3LYP²¹ functional, and aug-ss-pVDZ²² basis set. For comparison, a def2-TZVPP²³ basis set was also used. A D3BJ²⁴ dispersion correction was employed. All systems were fully relaxed. Activation barriers were computed through surface scans of saddle-point optimizations. Vibrational frequencies were analyzed through transition state optimizations with exact Hessian, recalculated every five steps. NEB calculations proceeded with xtb²⁵ binding and the vpo²⁶ algorithm of optimization. Lastly, a time-dependent DFT (TD-TPD) calculation was used to analyze excited states: the TD-DFT was carried out with 150 transitions and Davidson-expansion space 300. Visualizations were carried out on Chemcraft²⁷ quantum chemistry software.

Experimentally, a 254 nm mercury lamp (UVP R-52g, power 100 W) was used for an investigation of the UV effect. The lamp illuminated the cyclic voltammetry synthesis process, as detailed previously¹⁹. For comparison, a 365 nm mercury lamp (UVP B-100AR, power 100W) was also used. Temperature-programmed desorption (TPD) was used to measure the PN yield. Fourier transform infrared (FTIR) and Raman spectroscopy were used to confirm the PN synthesis.

Raman spectroscopy was performed with a Thermo Scientific DXR Raman microscope. FTIR was carried out using a Nicolet ThermoElectron FTIR spectrometer combined with a MIRacle ATR platform assembly and a ZnSe plate, and denoted as ATR-FTIR. TPD was carried out using the AutoChem II 2920 system. Samples were heated in flowing helium from room temperature to 850 °C at a heating rate of 10 °C /min. The released species were monitored with an on-line mass spectrometer (QMS 200, Stanford Research Systems).

3. Results and discussion

A full geometric optimization of an azide radical (N_3^*) and anion (N_3^-) were first investigated (Fig. 1a). The Gibbs free energy of the azide anion is lower than the azide radical by 60 kcal/mol. Two azide radical molecules were then optimized in a variety of configurations to form an N_6 molecule. In each case, the system converged to the configuration in Fig 1b. A numerical frequency calculation then confirmed that N_6 is a stable intermediate (Table S1). This configuration is in agreement with the lowest-energy N_6 found by Greschner *et al.*²⁸. Following this, two N_6 molecules were combined into a variety of configurations to create an N_{12} molecule. Only two of these configurations are stable, while all others decompose. Of these two, the lowest energy N_{12} configuration adopted a zigzag configuration (Fig 1c); the metastable state is shown in Figure S1.

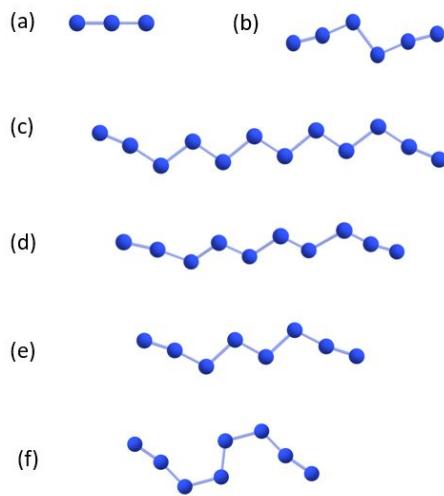


Figure 1: Lowest energy structures of: a) N_3^* b) N_6 c) N_{12} d) N_{10} e) EEE N_8 and f) ZEZ N_8

All possible pathways from N_{12} to N_8 were then examined. In agreement with a DFT study by Battaglia *et al.*¹², N_5 was found to be unstable, decomposing into $\text{N}_3 + \text{N}_2$. Thus, it was necessary to discard any pathway based on N_5 , such as $\text{N}_{12} \rightarrow \text{N}_9 + \text{N}_3 \rightarrow \text{N}_7 + \text{N}_2 + \text{N}_3 \rightarrow \text{N}_5 + \text{N}_2 + \text{N}_2 + \text{N}_3 \rightarrow \dots \text{N}_8$. Similarly, any pathway that builds on N_2 as a reactant was discarded, as diatomic nitrogen is inert under atmosphere condition¹. Additionally, N_4 was found to decompose to N_2 except in square or chain configurations; however, as neither of these configurations will react to build N_8 but will decompose, any pathway based on N_4 was also discarded. Lastly, any pathway using monatomic nitrogen was excluded.

The remaining two possibilities are from N_{12} to N_8 directly, or to $\text{N}_{10} + \text{N}_2$ and then to $\text{N}_8 + 2\text{N}_2$. To clarify either pathways, a saddle point optimization was carried out with relaxed scan to find the minimum energy path to the transition state, in an eigenvector-following calculation²⁰. As N_{12} dissociating into $\text{N}_{10} + \text{N}_2$ has a much lower energy barrier (5 kcal/mol) compared to the direct decomposition of N_{12} to $\text{N}_8 + 2\text{N}_2$ (60 kcal/mol barrier), it is the probable synthesis mechanism. Fig 1d and 1e show the optimized N_{10} configuration and the resulting N_8 configuration, respectively. Finally, this neutral N_8 molecule will reconfigure to N_8^- (Fig. 1f) upon reduction; N_8^- molecule has a lower in energy than N_8 by 32 kcal/mol. Compared to the EEE N_8 cleaved from N_{10} , the ZEZ configuration contains one shifted atom, as seen in Fig 1d. From a nudged elastic band (NEB) calculation, it is found that this reconfiguration is nearly spontaneous with an energy barrier of only 3 kcal/mol (Fig S2).

To determine the full synthesis mechanism, a saddle point was optimized with relaxed scan for each step leading to N_8 in order to determine the transition states. The vibrational frequencies for each step were calculated numerically; for stability, there must be no negative vibrational frequencies, while transition states exhibit one negative frequency. From N_3 to N_6 , the scan consisted of decreasing the distance between two N_3 molecules (specifically atom N1 and N6, Figure S3) from 3 Å to 1 Å. It was found that the formation of N_6 from $2N_3$ is spontaneous.

Similarly, the N_{12} scan consisted of decreasing the distance between two N_6 molecules from 3 Å to 1 Å. From the scan, the transition state was identified (TS1, Fig. 2a); an optimization and subsequent numerical frequency calculation showed only one negative frequency, confirming this to be the transition state between N_6 and N_{12} (Table S1). The process from N_6 to N_{12} requires overcoming this transition state with an activation barrier of 51 kcal/mol. Similarly, the transition state from the decomposition of N_{12} to N_{10} was identified and shown in Fig. 2b. Again, an optimization and numerical frequency calculation confirm this transition state (Table S1). From N_{12} to N_{10} , the activation barrier is about 10 kcal/mol. Finally, from N_{10} to N_8 , the transition state (Fig. 2c) energy barrier is about 15 kcal/mol. These values are relatively low and can easily be overcome by the cyclic voltammetry process. It is likely that plasma methods of fabrication would provide even more energy input, rendering these two activation barriers moot. The last step is the reduction and reconfiguration of N_8 to N_8^- . The Gibbs free energy reaction diagram for the entire aforementioned synthesis mechanism, from the azide anion to the neutral N_8 , is shown in Fig. 3. The radicalization of azide does not require a conformational change, and so the difference in the single point energies indicates the radicalization energy, about 60 kcal/mol. As this quantity is the highest in the mechanism, it is the rate-limiting step. Finally, to demonstrate that the predictions were independent of the basis set choice, a TZVPP basis set was used to compare with the aug-ss-pVDZ. The TZVPP set has extended polarizability functions, which can be useful in analyzing the negative charge of N_8^- . As shown in the Supplementary Information, the energy differences are very similar, confirming the validity of the calculated pathway.

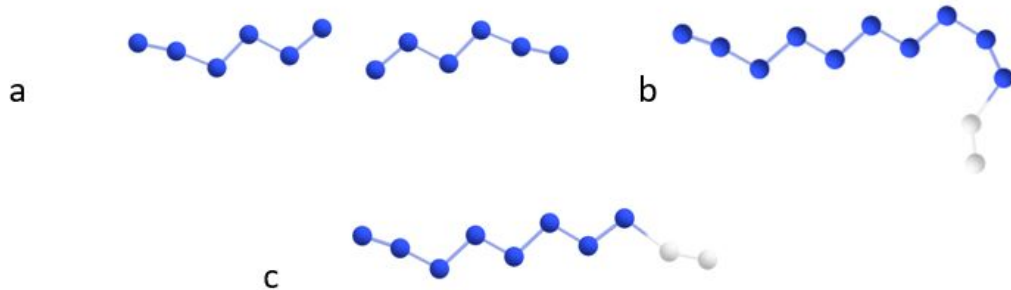


Fig 2: a) Transition state between N_6 and N_{12} (TS 1). b) Transition state between N_{12} and N_{10} (TS 2). c) Transition state between N_{10} and N_8 (TS 3). Dissociating N atoms are in gray.

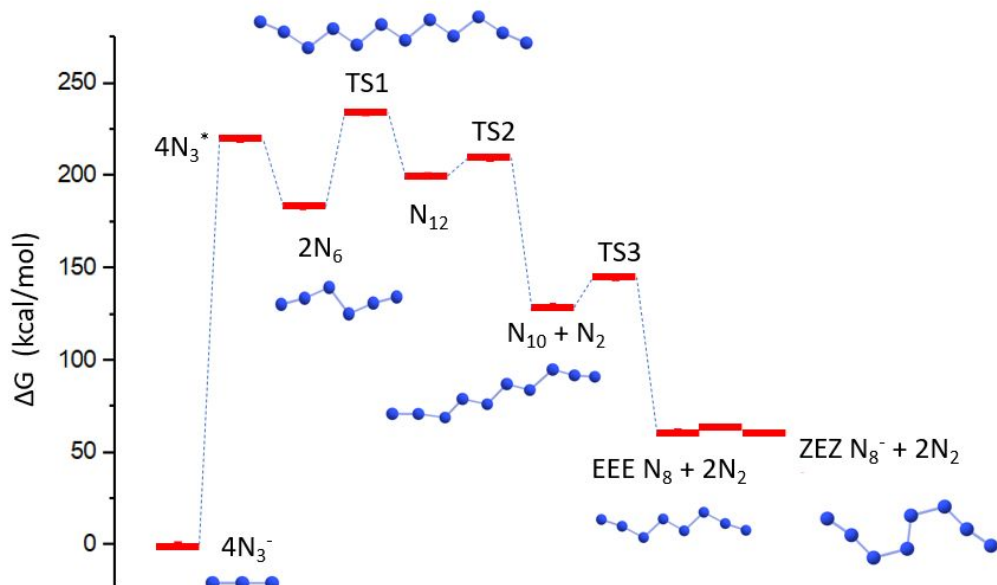


Fig 3: Reaction diagram for the synthesis mechanism of N_8^- from N_3^- precursor

Based on the above mechanism, the rate-limiting step of the whole mechanism, N_3^- to N_3^* with 60 kcal/mol energy barrier, controls the yield of PN synthesis. Thus, increasing the rate of oxidizing N_3^- to N_3^* would enhance the yield of PN product. A time-dependent DFT (TD-DFT) calculation was performed on the azide ion to analyze the excitation states in this rate-limiting step. The calculated UV spectrum shows peaks at 150, 233 and 290 nm (Fig 4). This prediction indicates that exposing the azide to radiation of about 233 nm would likely enhance the

conversion of N_3^- to N_3^* . To confirm this, PN was synthesized following the same cyclic voltammetry (CV) procedure as the work from Wu *et al.*,¹⁹ but under UV irradiation with a wavelength of 254 nm within the absorption band. For comparison, the PN synthesis was also carried out under 365 nm light, which would not be adsorbed according to the TD-DFT calculations. The quantity of PN was determined with TPD measurements, and the yield increases by about four times under UV irradiation, as shown in Table 1. In comparison, the amount of sample from 365 nm UV light irradiation does not increase, but instead decreases slightly due to the thermal effect. The result demonstrates that UV illumination combined with CV is a promising way to produce this PN species.

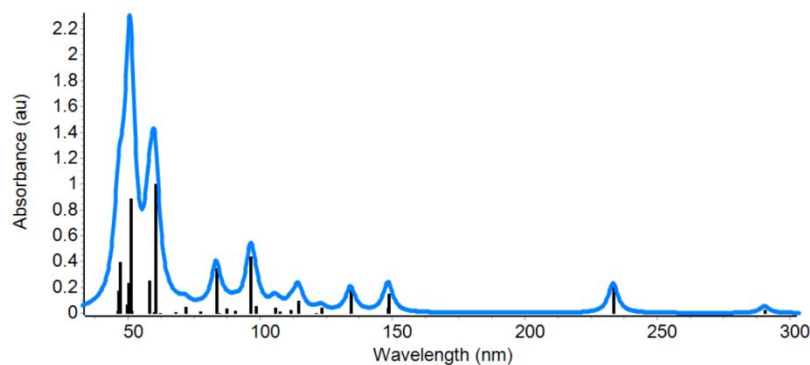


Fig 4: TD-DFT of absorption spectra for N_3^-

Table 1: PN yield enhancement under UV light.

Sample	Nitrogen Desorption Amount (mmol/g)
PN-MWNT	1
PN-MWNT 254 nm	3.9
PN-MWNT 365 nm	0.9

The resulting PN produced from these CV experiments were characterized with Raman and IR spectroscopy. DFT was used to predict the Raman and IR spectra of each PN molecule; the peaks computed for the N_8 with a zigzag ZEZ configuration match the experiment results, as seen in Fig 5a and 5b, as well as Table 2. These values are in agreement with the previous work¹⁹: the 2059 IR peak matches the 2050 experimental peak, and the 1049 Raman peak

matches the 1080 experimental peak. The slight discrepancies could be attributed to solvation and thermal effects that were not included in the model.

Table 2: DFT vs Experimental Raman and IR major peaks

	Raman peaks	IR peaks
ZEZ DFT	1049	2059
Experiment	1080	2050

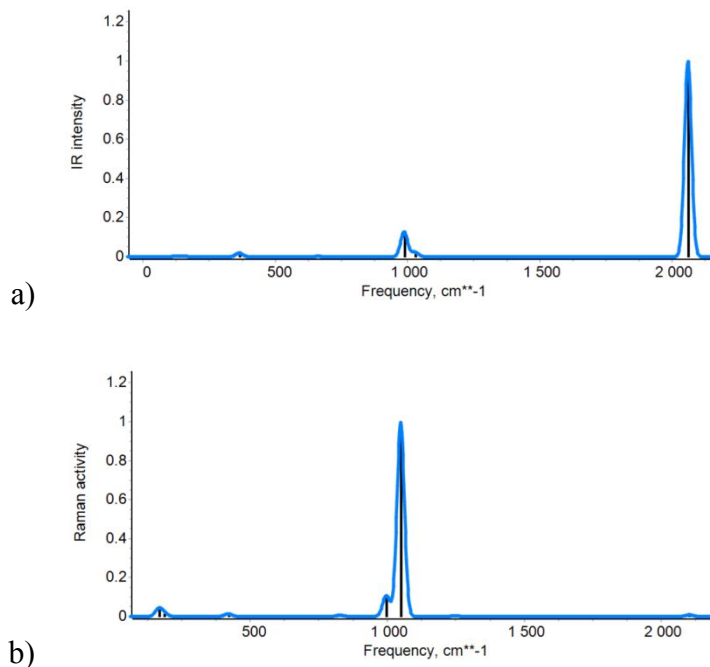


Fig 5. DFT calculated a) IR and b) Raman spectra of N_8^- .

These findings present a facile way to synthesize PN at ambient conditions. Conventional PN synthesis has consisted of N_2 precursors, a transformation which has required very high temperatures and pressures. For example, in a 2004 experiment by Eremets *et al.*, the cubic gauche (cg) form of PN was synthesized by laser heating molecular N_2 to a temperature of 2000 K at a pressure of 110 GPa in a diamond cell. In 2007, Gregoryanz *et al.*⁶ raised temperatures to 150 GPa and pressures to 2000 K, for a diamond cell system with N_2 precursors; they were able to construct a phase diagram for various PNs. In 2014, Tomasino *et al.*⁷ also used a diamond

anvil system with N₂ precursors, at pressures between 120 and 180 GPa and temperatures up to 3000 K, to produce the Pba2 phase of PN. Because of the very high energy barriers associated with breaking the bonds of N₂ to form single bonds in PN, these N₂ precursor methods require extreme conditions. A DFT study by Plašienka *et al.*²⁹ articulates the synthesis mechanism for transforming N₂ to cg PN at high temperature and pressure conditions, and found that it proceeds through a number of intermediate crystal structures only possible at high pressure.

In contrast, this study presents the synthesis of PN from an azide precursor, at ambient conditions. By explicating the synthesis mechanism in vacuum, this study shows the plausibility of producing PN with significantly less energy requirements. In fact, this synthesis mechanism has been shown to consist of several spontaneous and low activation energy steps, highlighting the facile nature of this synthesis method. Moreover, this synthesis mechanism indicates that whereas other PN stabilization methods have often involved substrate effects,^{2,8,10} the interactions of N₃, N₆, N₁₂ and N₁₀ isomers lead to the formation of N₈ without the need of a substrate.

Contrast with conventional energy-intensive methods, the synthesis mechanism here underpins the ease with which the yield can be enhanced through UV light exposure. While there has not been much information in published literature on increasing PN yield, it can be surmised that conventional synthesis methods would improve yield only with great difficulty, due to the high energy required in N₂ diamond anvil cell transformations. This study, on the other hand, demonstrates that yield can be enhanced in a simple and practical way. This UV light technique for enhancement adds to the appeal of the PN, which has been shown to rival platinum in ORR activity.¹⁹ PN is thus promising not only as a high energy-density material with excellent catalytic ability, but as a material that can be synthesized in a facile and scalable way, with a new mechanistic understanding of synthesis at ambient conditions.

4. Conclusion:

Using ab initio calculations, a practical and rational way to produce N₈⁻ PN from N₃⁻ is determined. The detailed mechanism is an intuitive and logical process of dissociating N₂ pairs from the endpoints of N₁₂ chains formed from N₆, which is in turn spontaneously formed from N₃ radicals. This study also explicates the energy barriers for each state, by calculating the saddlepoint optimizations, and for the last ionization step, an NEB value. The stability of each

state was confirmed and transition states were determined through vibrational frequency calculations. It was found that the radicalization of azide N_3^- is the rate limiting step. A TD-DFT calculation was used to calculate the absorbtion spectrum of N_3^- and predict a method of yield enhancement via illumination under UV light. An experiment confirmed this enhancement by a generating yield four times greater than without illumination. This understanding of the PN synthesis and approach to yield enhancement can be utilized to scale up production of this excellent catalytic material in applications such as fuel cells, where the PN can act as a cathodic catalyst.

Acknowledgements:

This work was supported by NSF CBET-1804949. Density functional theory calculations were performed using high performance computing clusters at the New Jersey Institute of Technology (“Kong” and “Lochness”).

Contributions:

S. Alzaim did the theoretical calculation and wrote the manuscript. Z. Wu did UV irradiation experiments. M. Benchafia helped S. Alzaim with initial FTIR and Raman calculation methods. J. Young guided S. Alzaim with different DFT methods. X. Wang supervised the students and led the research project. Both J. Young and X. Wang finalized the manuscript.

Data and materials availability: All data needed to evaluate the conclusions in the paper are present in the paper and/or the Supplementary Materials. Additional data related to this paper may be requested from the authors.

References:

- 1 Y. Li, X. Feng, H. Liu, J. Hao, S. A. T. Redfern, W. Lei, D. Liu and Y. Ma, Route to high-energy density polymeric nitrogen t-N via He-N compounds, *Nat. Commun.*, 2018, **9**, 1–7.
- 2 S. Niu, S. Liu, B. Liu, X. Shi, S. Liu, R. Liu, M. Yao, T. Cui and B. Liu, High energetic polymeric nitrogen sheet confined in a graphene matrix, *RSC Adv.*, 2018, **8**, 30912–30918.
- 3 Y. Li, H. Bai, F. Lin and Y. Huang, Energetics and electronic structures of nitrogen chains encapsulated in zigzag carbon nanotube, *Phys. E Low-Dimensional Syst. Nanostructures*, 2018, **103**, 444–451.
- 4 X. Li, *Principles of fuel cells*, CRC Press, 2005.

- 5 M. I. Eremets, A. G. Gavriliuk, I. A. Trojan, D. A. Dzivenko and R. Boehler, Single-bonded cubic form of nitrogen, *Nat. Mater.*, 2004, **3**, 558–563.
- 6 E. Gregoryanz, A. F. Goncharov, C. Sanloup, M. Somayazulu, H. K. Mao and R. J. Hemley, High P-T transformations of nitrogen to 170 GPa, *J. Chem. Phys.*, , DOI:10.1063/1.2723069.
- 7 D. Tomasino, M. Kim, J. Smith and C. S. Yoo, Pressure-induced symmetry-lowering transition in dense nitrogen to layered polymeric nitrogen (LP-N) with colossal raman intensity, *Phys. Rev. Lett.*, 2014, **113**, 1–5.
- 8 H. Abou-Rachid, A. Hu, V. Timoshevskii, Y. Song and L. S. Lussier, Nanoscale high energetic materials: A polymeric nitrogen chain N8 confined inside a carbon nanotube, *Phys. Rev. Lett.*, 2008, **100**, 1–4.
- 9 W. Ji, V. Timoshevskii, H. Guo, H. Abou-Rachid and L. Lussier, Thermal stability and formation barrier of a high-energetic material N 8 polymer nitrogen encapsulated in (5,5) carbon nanotube, *Appl. Phys. Lett.*, 2009, **95**, 10–13.
- 10 V. Timoshevskii, W. Ji, H. Abou-Rachid, L. S. Lussier and H. Guo, Polymeric nitrogen in a graphene matrix: An ab initio study, *Phys. Rev. B - Condens. Matter Mater. Phys.*, 2009, **80**, 1–5.
- 11 B. Hirshberg, R. B. Gerber and A. I. Krylov, Calculations predict a stable molecular crystal of N8, *Nat. Chem.*, 2014, **6**, 52–56.
- 12 S. Battaglia, S. Evangelisti, T. Leininger and N. Faginas-Lago, in *International Conference on Computational Science and Its Applications*, 2018, pp. 579–592.
- 13 R. J. Bartlett, Structure and Stability of Polynitrogen Molecules and their Spectroscopic Characteristics, 2002, **8435**, 1–93.
- 14 F. Barat, B. Hickel and J. Sutton, Flash photolysis of aqueous solutions of azide and nitrate ions, *J. Chem. Soc. D Chem. Commun.*, 1969, 125b–126.
- 15 A. Treinin and E. Hayon, Spectroscopic observation of the azide radical in solution, *J. Chem. Phys.*, 1969, **50**, 538–539.
- 16 E. Hayon and M. Simic, Absorption spectra and kinetics of the intermediate produced from the decay of azide radicals, *J. Am. Chem. Soc.*, 1970, **92**, 7486–7487.
- 17 S. M. Peiris and T. P. Russell, Photolysis of compressed sodium azide (NaN3) as a synthetic pathway to nitrogen materials, *J. Phys. Chem. A*, 2003, **107**, 944–947.

18 N. Holtgrewe, S. S. Lobanov, M. F. Mahmood and A. F. Goncharov, Photochemistry within compressed sodium azide, *J. Phys. Chem. C*, 2016, **120**, 28176–28185.

19 Z. Wu, E. M. Benchafia, Z. Iqbal and X. Wang, N8 polynitrogen stabilized on multi-wall carbon nanotubes for oxygen-reduction reactions at ambient conditions, *Angew. Chemie - Int. Ed.*, 2014, **53**, 12555–12559.

20 F. Neese, Software update: the ORCA program system, version 4.0, *Wiley Interdiscip. Rev. Comput. Mol. Sci.*, 2018, **8**, e1327.

21 A. Schäfer, H. Horn and R. Ahlrichs, Fully optimized contracted Gaussian basis sets for atoms Li to Kr, *J. Chem. Phys.*, 1992, **97**, 2571–2577.

22 T. H. Dunning Jr, Gaussian basis sets for use in correlated molecular calculations. I. The atoms boron through neon and hydrogen, *J. Chem. Phys.*, 1989, **90**, 1007–1023.

23 A. D. Becke, Becke's three parameter hybrid method using the LYP correlation functional, *J. Chem. Phys.*, 1993, **98**, 5648–5652.

24 S. Grimme, J. Antony, S. Ehrlich and H. Krieg, A consistent and accurate ab initio parametrization of density functional dispersion correction (DFT-D) for the 94 elements H-Pu, *J. Chem. Phys.*, 2010, **132**, 154104.

25 J. Jenke, A. N. Ladines, T. Hammerschmidt, D. G. Pettifor and R. Drautz, Tight-binding bond parameters for dimers across the periodic table from density-functional theory, 2019, 1–12.

26 S. Grimme, Exploration of Chemical Compound, Conformer, and Reaction Space with Meta-Dynamics Simulations Based on Tight-Binding Quantum Chemical Calculations, *J. Chem. Theory Comput.*, 2019, **15**, 2847–2862.

27 G. A. Zhurko, ChemCraft Software. 2019.

28 M. J. Greschner, M. Zhang, A. Majumdar, H. Liu, F. Peng, J. S. Tse and Y. Yao, A New Allotrope of Nitrogen as High-Energy Density Material, *J. Phys. Chem. A*, 2016, **120**, 2920–2925.

29 D. Plašienka and R. Martoňák, Transformation pathways in high-pressure solid nitrogen: From molecular N₂ to polymeric cg-N, *J. Chem. Phys.*, 2015, **142**, 1–10.

Supplementary Information:

Calculations guide a practical way to synthesize N_8 polymeric nitrogen from N_3^- precursor

Safa Alzaim, Zhiyi Wu, Mostafa Benchafia, Joshua Young,* Xianqin Wang*

Dept. of Chemical and Materials Engineering, New Jersey Institute of Technology, Newark, NJ, 07102, USA

Corresponding author: jyoung@njit.edu; xianqin.wang@njit.edu

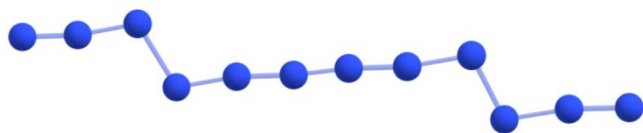


Fig S1: $2N_3$ metastable state to N_{12}

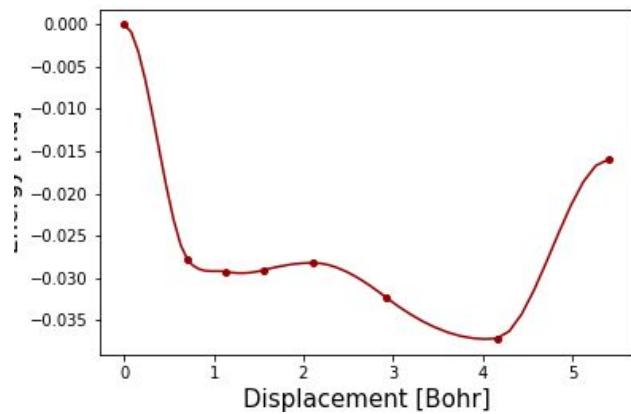


Fig S2: NEB for EEE N_8^* to ZEZ N_8^-

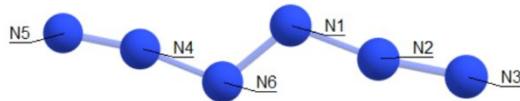


Fig S3: Two azides to form N₆

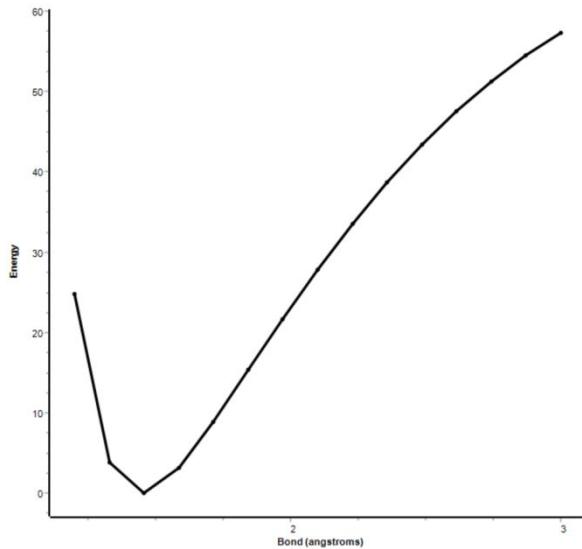


Fig S4: N₃ to N₆ Saddlepoint Surface Scan

Table S1: Vibrational Frequencies of Transition States

Transition State	Vibrational Frequency for Imaginary Mode (cm**-1)
N6 to N12	-550.6
N12 to N10	-625.4
N10 to N8	-729.59

Table S2: Gibbs free energies for TZVPP and aug-ss-pVDZ basis sets

	aug (ht)	TZVPP (ht)
N2	-109.504	-109.535
N3-	-164.171	-164.231
N3rad	-164.076	-164.144
N6	-328.231	-328.317
TSN6_N12	-656.39	-656.552
N12	-656.45	-656.608
N12toN10	-656.436	-656.592
N10	-547.051	-547.185
TSN10_N8	-547.027	-547.16
N8fN10	437.6481	-437.758
N8rad	-437.641	-437.74
N8minus	-437.688	-437.79